



## BIOCHAR FROM PALM KERNEL SHELL AND ITS APPLICATION FOR CU<sup>2+</sup> SORPTION

I Nyoman Candra<sup>1\*</sup>, Irma Sari<sup>2</sup>, Rosazlin Abdullah<sup>3</sup>, Rina Elvia<sup>4</sup> and Dewi Handayani<sup>5</sup>

<sup>1,3,5,4</sup> Study Program of Chemistry Education, Faculty of Education and Teacher Training, University of Bengkulu, Bengkulu 38371A, Indonesia.

<sup>2</sup> Institute of Biological Sciences, Universiti Malaya, 50603 Kuala Lumpur, Malaysia.

Corresponding E-mail: [inyomancandra@unib.ac.id](mailto:inyomancandra@unib.ac.id)

**Abstract:** Oil palm kernel shells (KS) are a byproduct of oil palm processing that often receives little attention and is treated as waste. Biochar has various applications for example as an adsorbent. This study aims to prepare and characterize biochar from KS and evaluate its effectiveness in adsorbing Cu<sup>2+</sup>. The biochar (BKS) was prepared by heating KS in a furnace at 500°C for three hours. The resulting material was sieved using a 50-mesh sieve to ensure uniformity. Characterization of BKS showed that it had a surface area of 319.9 m<sup>2</sup> g<sup>-1</sup>, a total pore volume of 0.168 cm<sup>3</sup> g<sup>-1</sup>, and an average pore size of 1.049 nm, classifying it as microporous. Analysis for its functional groups revealed the presence of functional groups with stretching vibrations corresponding to O-H (3400 cm<sup>-1</sup>), C-H (2920 cm<sup>-1</sup>), C=O (1700 cm<sup>-1</sup>), C=C (1432-1690 cm<sup>-1</sup>), and C-O (1000-1200 cm<sup>-1</sup>). SEM imaging displayed a clear porous structure with well-defined channels. Adsorption isotherm experiments demonstrated that Cu<sup>2+</sup> adsorption data using BKS aligned better with the Freundlich isotherm model than with the Langmuir model. These findings indicate that BKS derived from KS is less effective for removing Cu<sup>2+</sup> ions from water compared to other biochars..

**Keywords:** Environment, Environmental Pollution, Garbage, Waste

### How to cite this article :

Candra, I., Sari, I., Abdullah, R., Elvia, R., & Handayani, D. (2025). Biochar From Palm Kernel Shell and Its Application For CU2+ Sorption. IJIS Edu : Indonesian Journal of Integrated Science Education, 8(1). doi:<http://dx.doi.org/10.29300/ijisedu.v8i1.9561>

## 1. Introduction

Palm oil is a key commodity in Indonesia's agriculture and plantation sectors, particularly in Bengkulu Province. In 2021, it produced approximately 189.87 thousand tons of palm oil (BPS, 2021). This production is accompanied by a large quantity of KS, which have received little attention and are often discarded as waste without further utilization. Many researches have been conducted to explore the potential of transforming KS into high-performance materials.

As a biomass material, KS has a high carbon content, making it a promising candidate for conversion into biochar. Biochar is a highly porous charcoal material produced by heating biomass, a process that burns away non-carbon substances such as cellulose and lignin, leaving behind pure carbon. It has a broad spectrum of applications, including as a catalyst (Yuan et al., 2023), electrode (Sangrulkar et al., 2023), and adsorbent (Ji et al., 2024); (Liu et al., 2021); (Yao et al., 2021).

The performance of biochar as an adsorbent depends largely on several parameters that influence its ability to absorb adsorbates, such as surface area and porosity. A high surface area and porosity allow biochar to adsorb larger amounts of adsorbate. Additionally, the functional groups present on biochar play a key role in its adsorption capacity. Therefore, analyzing surface area, porosity, and functional groups is crucial when using biochar as an adsorbent.

$\text{Cu}^{2+}$  is a common pollutant found in both water and drinking water. Numerous studies have reported  $\text{Cu}^{2+}$  ion contamination in water bodies. It is also known that  $\text{Cu}^{2+}$  can have adverse effects on human health, such as causing digestive issues and enzyme functionality. Sources of  $\text{Cu}^{2+}$  include pigments, plant enrichers, chemical agents, and Steel production plants. The concentration of  $\text{Cu}^{2+}$  ions has significantly increased in both local and global water environments.

This research is conducted in response to the issues mentioned above and the limited studies on the production and characterization of biochar from KS, as well as its application for removing  $\text{Cu}^{2+}$  from water.

## 2. Method

### Materials

KS was obtained from PT Agricinal Company in North Bengkulu Regency. Copper sulfate pentahydrate ( $\text{CuSO}_4 \cdot 5\text{H}_2\text{O}$ ) and hydrochloric acid (HCl) used in this study were purchased from Merck (Germany) and Sigma-Aldrih (USA) respectively.

### Biochar preparation

The dried KS was heated in an oven at a rate of  $10^\circ\text{C}$  per minute, reaching a maximum temperature of  $500^\circ\text{C}$  and maintained for three hours. The resulting biochar (BKS) was then sieved using a 50-mesh sieve to ensure uniform particle size.

### Biochar characterization

The sieved BKS was characterized using the Brunauer-Emmett-Teller (BET) method to determine its surface area and porosity. Functional groups were identified using FTIR, while SEM was utilized to examine the biochar's surface morphology.

### Biochars application for removing $\text{Cu}^{2+}$ ion from water

The adsorption experiment of  $\text{Cu}^{2+}$  using BKS was performed using a batch adsorption method. In this procedure, 2.5 g of biochar was introduced into each of four 60 mL polyethylene bottles, followed by the addition of 47, 46.5, 45.5, and 43.5 mL of distilled water, respectively. The pH of the biochar–distilled water mixtures in the bottles was adjusted to 5.5 using HCl 0.1M. The mixtures were then pre-equilibrated by shaking on a shaker for 24 hours.

After pre-equilibration, specific volumes (0.5, 1, 2, and 4 mL) of a 100 ppm  $\text{Cu}^{2+}$  stock solution were spiked to the bottles to obtain final  $\text{Cu}^{2+}$  concentrations of 1, 2, 4, and 8 ppm, respectively. The mixtures were then shaken for an additional 24 hours to reach equilibrium. Finally, the mixtures were filtered, and the remaining  $\text{Cu}^{2+}$  concentrations in the filtrates were measured using a UV-Visible spectrophotometer.

## Data analysis

The remaining  $\text{Cu}^{2+}$  concentration in the filtrate was used to calculate the amount of  $\text{Cu}^{2+}$  adsorbed by the biochar. The adsorption behavior of  $\text{Cu}^{2+}$  onto BKS was evaluated using the Langmuir and Freundlich isotherm models. The Langmuir isotherm equation is expressed as follows:

$$\frac{1}{q_e} = \frac{1}{q_{max}} + \frac{1}{K_L q_{max} C_e}$$

When the both sides are multiplied by  $C_e$ , the following equation is obtained.

$$\frac{C_e}{q_e} = \frac{C_e}{q_{max}} + \frac{1}{K_L q_{max}}$$

Where  $q_e$  =  $\text{Cu}^{2+}$  adsorbed on the biochars (mg/g);  $C_e$  = equilibrium concentration of  $\text{Cu}^{2+}$  in the solution (mg/L);  $q_{max}$  = maximum capacity of biochars (mg/g) and  $K_L$  = Langmuir constant. In order to obtain  $q_{max}$  and  $K_L$ , plotting  $C_e/q_e$  vs  $C_e$  was performed. Whereas, for Freundlich isotherm, adsorption of  $\text{Cu}^{2+}$  onto BKS was analyzed according to the following equation.

$$\log q_e = \log K_F + 1/n \log C_e$$

with  $K_F$  and  $n$  are Freundlich constant.

## 3. Result and Discussion

### Preparation and characterization of biochar

The biochar produced from palm kernel shell is shown in Figure 1. The biochar exhibited a durable and robust physical texture, attributed to its high carbon content from lignin, cellulose, and hemicellulose (Wang et al., 2021). Furthermore, Mansyur et al. (2022) suggested that this physical characteristic is due to its high aromatic carbon content and well-crystallized mineral structure.



Figure 1. The biochar before grinded (a); grinding process of the biochar (b); Sieved biochar (c)

Characterization of biochar using BET methode found that its specific surface area, total pore volume and pore size were  $319.9 \text{ m}^2 \cdot \text{g}^{-1}$ ,  $0.168 \text{ cm}^3 \cdot \text{g}^{-1}$ , and  $1.049 \text{ nm}$ , respectively. The pore size of the biochar ( $< 2 \text{ nm}$ ) is chatagorized as micropore (Leng et al., 2021). BET curve of the biochar is depicted in Figure 2.

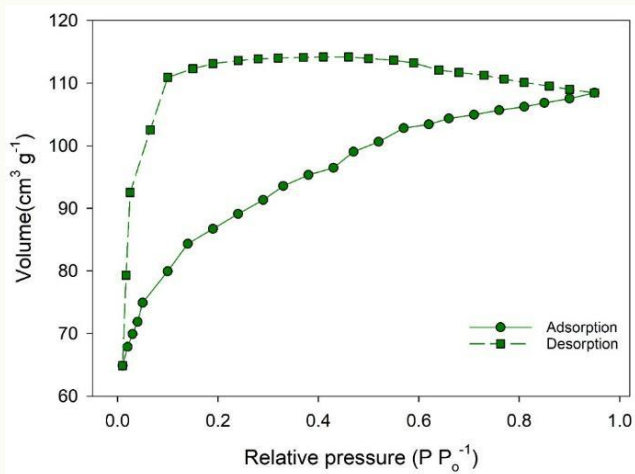


Figure 2. BET curve of biochar from oil palm kernel shell

The surface area of the biochar in this work was higher than that reported in other studies (Table 1). The temperature applied during biochar preparation plays a vital role in determining its specific surface area. It is well - known that increasing the heating temperature alters the specific surface area and porosity due to the breakdown of organic material and the formation of micropores (Yang et al., 2021).

Table 1: Specific surface area, total volume and pore size of biochar from oil palm kernel shell obtained in this study and others researches

Temp. (°C)	Duration (hour)	Heating rate (°C min <sup>-1</sup> )	Specific surface area (m <sup>2</sup> g <sup>-1</sup> )	Total volume (cm <sup>3</sup> g <sup>-1</sup> )	Pore size (nm)	Sources
450	1	10	36.33	0.039	28.22	Ma et al.(2017)
500	1	10	191	-	-	Lee et al.(2013)
500	1	-	208	0.21	-	Kong et al. (2019)
500	0.5	-	268	0.24	-	Kong et al. (2019)
500	1.5	-	238	0.29	-	Kong et al. (2019)
<b>500</b>	<b>3</b>	<b>10</b>	<b>319.9</b>	<b>0.168</b>	<b>1.049</b>	<b>This study</b>
550	1	10	98.81	0.055	23.26	Ma et al.(2017)
600	1	5	220	0.16	-	Windeatt et al. (2014)
700	3	10	90.02	0.053	2.36	Hamza et al.(2016)

note: \*Heating duration at final temperature; Temp.= temperature

According to Cárdenas-Aguiar et al. (2017), during biochar production, some processes occur as the temperature increases, covering: (1) water dehydration and removal of organic volatile compounds with small molecular weight at up to 200°C, (2) the breakdown of hemicellulosic and cellulosic materials at temperature ranging from 200°C to 500°C, and (3) the disintegration of lignin and other organic materials with strong chemical bonds at temperature more than 500°C. However, excessively high temperatures can collapse the pore structure, resulting in a decrease in specific surface area. As shown in Table 1, biochar prepared at 550°C, 600°C, and 700°C had a lower specific surface area compared to that prepared at 500°C in this study.

In addition to temperature, heating time is another crucial factor influencing the specific surface area of biochar. The same heating temperature with different heating durations can produce biochars with varying specific surface areas. Other parameters related to specific surface area include total pore volume and pore size. As presented

in Table 1, while the biochar in this study exhibited a higher specific surface area compared to other studies, it had a lower total pore volume and pore size.

Total pore volume represents the cumulative volume of all pores, primarily mesopores and macropores, in the biochar. Although micropores contribute less to total pore volume, they play a dominant role in influencing the surface area of the biochar (Leng et al., 2021).

The FTIR spectrum of the biochar is presented in Figure 3. The elucidation of functional groups on the biochar through FTIR analysis revealed a broad band between 3200 and 3500  $\text{cm}^{-1}$ , associated with the stretching vibration of O-H in alcohols and phenols, consistent with findings from other studies (e.g., Hamza et al., 2016; Pasieczna-Patkowska et al., 2025). The spectrum also exhibited a peak at 2920  $\text{cm}^{-1}$ , corresponding to C-H stretching vibrations, primarily originating from aliphatic -CH<sub>2</sub> and alkane -CH<sub>3</sub> groups. A peak between 1650 and 1850  $\text{cm}^{-1}$  was detected, attributed to the C=O stretching of aromatic rings. Additionally, a band at 1580  $\text{cm}^{-1}$  was observed, which is linked to the C=O bond in -COOH groups (Guan et al., 2025). The presence of C-H deformation from alkanes or alkyl group bending was indicated by a peak at 1436  $\text{cm}^{-1}$  (Armah et al., 2024). Furthermore, a peak at 1080  $\text{cm}^{-1}$  identified the C-O-C stretching of ether groups.

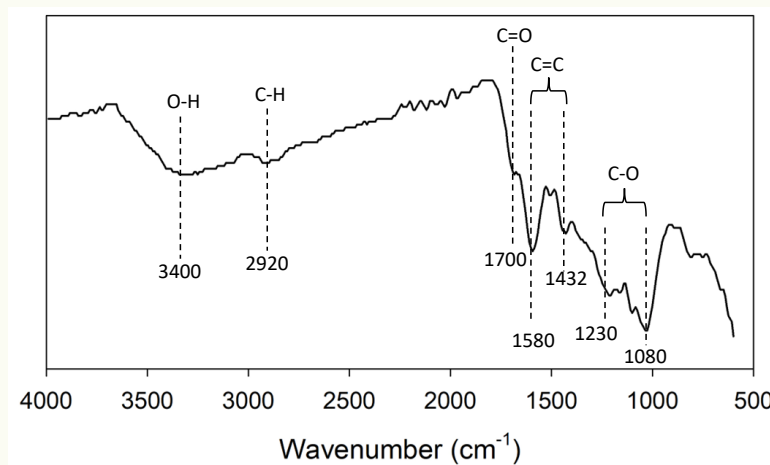


Figure 3: FTIR spectrum of biochar from oil palm kernel shell

The results of the biochar characterization using SEM are presented in Figure 4. The images reveal that the biochar surface possesses a mixed and highly complex network of pores, channels, and fibrous ridged structures, consistent with findings reported by (Saleh et al., 2025).

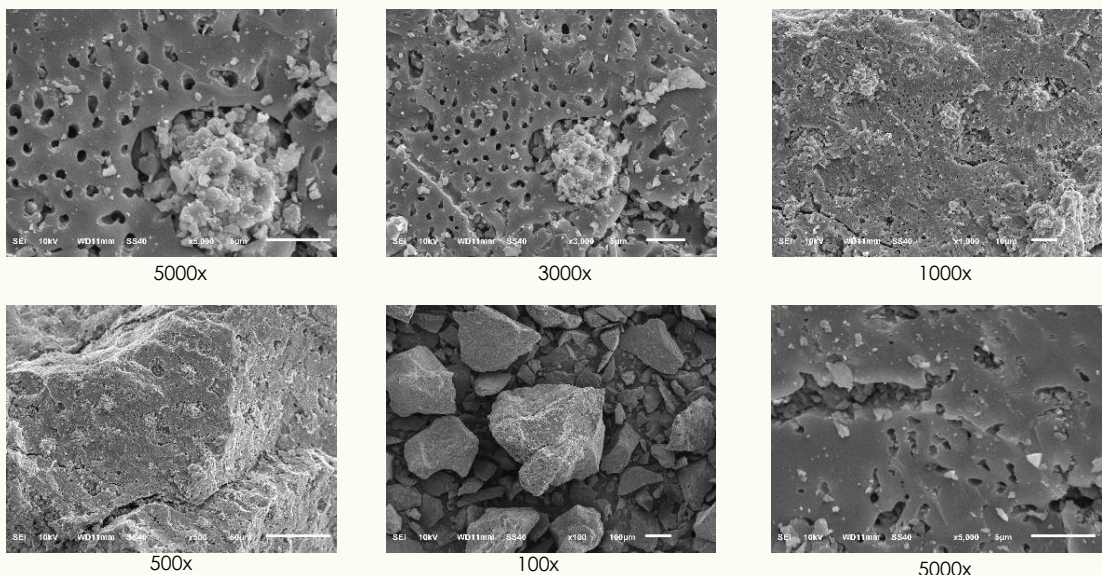


Figure 4: SEM images of the biochar with different magnification

**Adsorption** . This type of adsorption isotherm is characterized by an almost completely flat plateau at the saturation point of  $\text{Cu}^{2+}$  concentration in the solution (Brião et al., 2022). According to Kolesnikov et al. (2021), such an adsorption pattern is typical for microporous solids, where a strong interaction exists between the adsorbate and the adsorbent - in this case, the interaction between  $\text{Cu}^{2+}$  ions and the biochar.

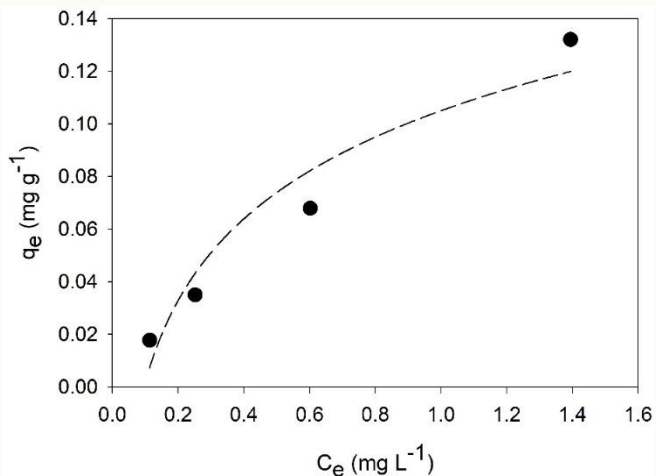


Figure 5: Adsorption isotherm of  $\text{Cu}^{2+}$  using biochar from oil palm kernel shell;  $C_e$  and  $q_e$  are concentration of  $\text{Cu}^{2+}$  in the solution and on the biochar, respectively, under equilibrium conditions.

Fitting of the adsorption data to the tested Langmuir and Freundlich isotherm models showed that both had almost the same  $R^2$ , indicating that they conformed suitably to the data. It can be concluded that the data fit well at the borderline between the Langmuir and Freundlich models, with  $R^2$  values of 0.95 and 0.999, respectively (Figure 6).

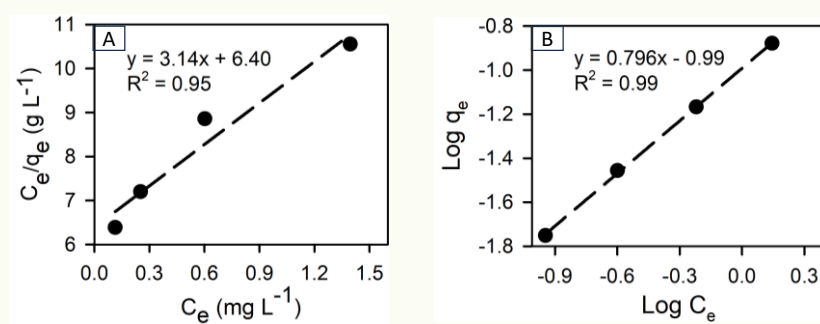


Figure 6. Data of  $\text{Cu}^{2+}$  adsorption using biochar from oil palm kernel shell fitted to Langmuir (A) and Freundlich (B) model

From the equation obtained by plotting the data to Langmuir and Freundlich Models, their parameters ( $q_{\max}$ ,  $K_L$ ,  $K_F$  and  $n$ ) were calculated. Langmuir and Freundlich parameters are presented in Table 2.

Table 2. Langmuir and Freundlich parameters for  $\text{Cu}^{2+}$  adsorption using biochar from oil palm kernel shell

Parameters	Model	
	Langmuir	Freundlich
$q_{\max}$ (mg g <sup>-1</sup> )	0.318	-
$K_L$ (L.mg <sup>-1</sup> )	0.49	-
$R^2$	0.95	
$K_F$	-	0.1
$n$	-	1.25
$R^2$	-	0.99

Maximum adsorption capacity of  $\text{Cu}^{2+}$  ( $q_{\max}$ ) using the biochar in this study was smaller (0.318 mg g<sup>-1</sup>) compared to adsorption of  $\text{Cu}^{2+}$  using other biochars, despite it had higher specific surface area. For example, adsorption of  $\text{Cu}^{2+}$  in aqueous solution using wheat straw biochar with specific surface area of 3.18 m<sup>2</sup> g<sup>-1</sup>, had the highest capacity of 8.8 mg g<sup>-1</sup> (Wang et al., 2022). Moreover, Kaya et al. (2020) reported maximum capacity of 14.73 mg g<sup>-1</sup> for adsorption of  $\text{Cu}^{2+}$  using biochar from Hazelnut whose specific surface area was 124.3 m<sup>2</sup> g<sup>-1</sup>. This showed that, besides specific surface area, other factors also determine maximum adsorption capacity of biochar for instance, functional groups. Pathirana et al. (2019) found that specific surface area is not the main factor, but surface functional groups are the key parameter influencing heavy metal adsorption capacity of adsorbent. Langmuir constant ( $K_L$ ) was higher compared to that reported in other researches, investigating  $\text{Cu}^{2+}$  adsorption using different biochar (i.e. Wang et al., 2022). This constant represents the affinity of the adsorbate for the adsorbent.

Freundlich constant ( $K_F$ ) represent adsorption capacity of adsorbent that is analogous to  $q_{\max}$  in the Langmuir isotherm. Other Freundlich parameters is  $n$ , indicating adsorption intensity and favorability. This parameter can be  $>1$ ,  $=1$ , or  $<1$ , indicating favorable adsorption, linear adsorption or unfavorable adsorption, respectively. When  $1/n$  close to 1, it indicates more uniform surface. In this study,  $n$  was 1.25, indicating favorable adsorption and suggesting a more homogenous surface.

#### 4. Conclusion

Biochar from unused waste material of oil palm kernel shell has been successfully prepared under temperature of 500°C for three hours. Characterization of the biochar showed clear pores and channel formation. The pore was classified as micropore that more contribute to the high specific surface area of the biochar. Despite having higher specific surface area, the biochar had lower maximum adsorption capacity, compared to other studies, investigating Cu<sup>2+</sup> adsorption using different biochar. However, specific surface area is not the main contributor governing maximum adsorption capacity. It was reported by other study that surface functional group was the key parameter influencing maximum adsorption capacity. Further investigation is required to explain why biochar with a high specific surface area has a low maximum adsorption capacity. Moreover, modifying biochar could potentially improve its maximum adsorption capacity.

#### Acknowledgments

We would like to express our gratitude to Institute for Research and Community Service, University of Bengkulu through Faculty of Education and Teacher Training for providing funding in this research. This research was conducted according to contract: 3730/UN30.7/PP/2024. We believe that this research would not have been possible without this financial support.

#### References

Armah, E. K., Chetty, M., Adedeji, J. A., Estrice, D. E., Mutsvene, B., Singh, N., & Tshemese, Z. (2023). Biochar: Production, Application. *Biochar: Productive Technologies, Properties and Applications*, 23.

Badan Pusat Statistik (BPS) Provinsi Bengkulu. (2021). Provinsi Bengkulu Dalam Angka. [www.bengkulu.bps.go.id](http://www.bengkulu.bps.go.id).

Brião, G. de, V., da Silva, M. G. C., Vieira, M. G. A., & Chu, K. H. (2022). Correlation of type II adsorption isotherms of water contaminants using modified BET equations. *Colloid and Interface Science Communications*, 46, 100557.

Cárdenas-Aguiar, E., Gascó, G., Paz-Ferreiro, J., & Méndez, A. (2017). The effect of biochar and compost from urban organic waste on plant biomass and properties of an artificially copper polluted soil. *International Biodeterioration & Biodegradation* 124: 223-232.

Guan, S., Liao, E., Sun, S., Peng, Q., Zeng, K., Shin, K., Guo, X., & Zhou, X. (2025). Raman spectroscopy. Energy Storage Materials Characterization: Determining Properties and Performance, 2, 397-417.

Hamza, U. D., Nasri, N. S., Amin, N. S., Mohammed, J., & Zain, H. M. (2016). Characteristics of oil palm shell biochar and activated carbon prepared at different carbonization times. Desalination and Water Treatment 57(17): 7999-8006.

Ji, G., Xing, Y., & You, T. (2024). Biochar as adsorbents for environmental microplastics and nanoplastics removal. Journal of Environmental Chemical Engineering, 12(5), 113377.

Kaya, N., Arslan, F., Yıldız Uzun, Z., & Ceylan, S. (2020). Kinetic and thermodynamic studies on the adsorption of Cu<sup>2+</sup> ions from aqueous solution by using agricultural waste-derived biochars. Water Supply, 20(8): 3120-3140.

Kolesnikov, A. L., Budkov, Y. A., & Gor, G. Y. (2021). Models of adsorption-induced deformation: ordered materials and beyond. Journal of Physics: Condensed Matter 34(6): 063002.

Kong, S. H., Loh, S. K., Bachmann, R. T., Zainal, H., & Cheong, K. Y. (2019). Palm kernel shell biochar production, characteristics and carbon sequestration potential. Journal of Oil Palm Research 31(3): 508-520.

Yuan, X., Cao, Y., Li, J., Patel, A. K., Dong, C. D., Jin, X., Gu, C., Yip, A.C.K., Tsang, D.C.W., & Ok, Y. S. (2023). Recent advancements and challenges in emerging applications of biochar-based catalysts. Biotechnology advances, 67, 108181.

Leng, L., Xiong, Q., Yang, L., Li, H., Zhou, Y., Zhang, W., Jiang, S., Li, H., & Huang, H. (2021). An overview on engineering the surface area and porosity of biochar. Science of the total Environment 763: 144204.

Liu, X. J., Li, M. F., & Singh, S. K. (2021). Manganese-modified lignin biochar as adsorbent for removal of methylene blue. journal of materials research and technology, 12, 1434-1445.

Ma, Z., Yang, Y., Ma, Q., Zhou, H., Luo, X., Liu, X., & Wang, S. (2017). Evolution of the chemical composition, functional group, pore structure and crystallographic structure of bio-char from palm kernel shell pyrolysis under different temperatures. Journal of Analytical and Applied Pyrolysis 127: 350-359.

Mansyur, N. I., Hanudin, E., Purwanto, B. H., & Utami, S. N. H. (2022). Chemical Properties and Micromorphology of Biochars Resulted from Pyrolysis of Agricultural Waste at Different Temperature. AGRIVITA Journal of Agricultural Science 44(3): 431-446.

Pathirana, C., Ziyath, A.M., Jinadasa, K., Egodawatta, P., Sarina, S., & Goonetilleke, A. (2019). Quantifying the influence of surface physico-chemical properties of biosorbents on heavy metal adsorption. Chemosphere 234: 488-495.

Pasieczna-Patkowska, S., Cichy, M., & Flieger, J. (2025). Application of Fourier

transform infrared (FTIR) spectroscopy in characterization of green synthesized nanoparticles. *Molecules*, 30(3), 684.

Saleh, A. M., Alias, A. B., Mahdi, H. H., Jawad, A. H., Syed-Hassan, S. S. A., Saleh, N. M., & Ahmed, O. K. (2024). Characterizing biochar derived from palm kernel shell biomass via slow pyrolysis for adsorption applications. *NTU Journal of Renewable Energy*, 6(1), 10-20.

Sangrulkar, P., Gupta, S., & Kandasubramanian, B. (2023). Advancements in biochar-based electrodes for improved performance of microbial fuel cells. *Bioresource Technology Reports*, 24, 101684.

Wang, S., Xiao, D., Zheng, X., Zheng, L., Yang, Y., Zhang, H., Ai, B., & Sheng, Z. (2021). Halloysite and coconut shell biochar magnetic composites for the sorption of Pb (II) in wastewater: synthesis, characterization and mechanism investigation. *Journal of Environmental Chemical Engineering* 9(6): 106865.

Wang, Y., Zheng, K., Jiao, Z., Zhan, W., Ge, S., Ning, S., Fang, S., & Ruan, X. (2022). Simultaneous removal of Cu<sup>2+</sup>, Cd<sup>2+</sup> and Pb<sup>2+</sup> by modified wheat straw biochar from aqueous solution: preparation, characterization and adsorption mechanism. *Toxics* 10(6): 316.

Windleatt, J. H., Ross, A. B., Williams, P. T., Forster, P. M., Nahil, M. A., & Singh, S. (2014). Characteristics of biochars from crop residues: potential for carbon sequestration and soil amendment. *Journal of environmental management* 146: 189-197.

Yang, C., Liu, J., & Lu, S. (2021). Pyrolysis temperature affects pore characteristics of rice straw and canola stalk biochars and biochar-amended soils. *Geoderma*, 397, 115097.

Yao, B., Luo, Z., Du, S., Yang, J., Zhi, D., & Zhou, Y. (2021). Sustainable biochar/MgFe<sub>2</sub>O<sub>4</sub> adsorbent for levofloxacin removal: Adsorption performances and mechanisms. *Bioresource Technology*, 340, 125698.